Biochemical and Biophysical Research Communications 447 (2014) 633–637

Contents lists available at ScienceDirect

Biochemical and Biophysical Research Communications

journal homepage: www.elsevier.com/locate/ybbrc

Regulatory effect of the glial Golli-BG21 protein on the full-length murine small C-terminal domain phosphatase (SCP1, or Golli-interacting protein)

Sergio Jaramillo-Tatis, Kenrick A. Vassall, Vladimir V. Bamm, George Harauz *

Department of Molecular and Cellular Biology, University of Guelph, 50 Stone Road East, Guelph, Ontario N1G 2W1, Canada

ARTICLE INFO

Article history:
Received 7 April 2014
Available online 18 April 2014

Keywords:
Golli (gene in the oligodendrocyte lineage)
Golli-interacting protein
Intrinsically-disordered protein
Myelin basic protein
Oligodendrocyte
Small C-terminal domain phosphatase

ABSTRACT

The gene in the oligodendrocyte lineage (*golli*) encodes a number of proteins essential for myelination, comprising Golli and classic isoforms that are expressed in a developmentally-regulated manner. The Golli-interacting-protein (GIP) was previously discovered in a search for potential interacting partners of the Golli-isoform BG21, and was realised to be an acidic phosphatase belonging to the family of RNA-polymerase-2, small-subunit, C-terminal phosphatases (*viz.*, SCP1). Here, we refer to this protein as mSCP1/GIP. In subsequent *in vitro* studies of recombinant murine SCP1/GIP, the inability to produce an active full-length version of the protein under native conditions necessitated the study of a truncated form ΔN-rmSCP1/GIP, but with inconclusive results regarding its interaction with BG21 [13]. We have since developed a new SUMO-expression and purification protocol for the preparation of a functional, full-length mGIP/SCP1, with no additional purification tags. Here, the interaction between mSCP1/GIP (with intact N-terminus) and BG21 is shown to be different than for the truncation mutant studied previously. Specifically, this interaction shows a dual effect on the enzymatic activity of mSCP1/GIP by BG21: BG21 enhanced mSCP1/GIP phosphatase activity (K_a = 30 μM), whereas PKCα-phosphorylated BG21 inhibited its activity (K_i = 2.9 μM), suggesting a potential role of BG21 as a molecular switch ("quick-brake mechanism") on mSCP1/GIP. The successful production of an active, full-length mSCP1/GIP thus demonstrates a role for its N-terminus in regulation of phosphatase activity, in events such as the regulation of transcription in oligodendrocytes.

1. Introduction

In the mammalian central nervous system, myelin is formed by oligodendrocytes, which arise from oligodendrocyte progenitor cells and proceed through a regulated differentiation pathway culminating in the assembly of the components of the compact myelin membrane [1,2]. Proteins encoded by the *golli* (***g***ene in the ***ol***igodendrocyte ***li***neage) complex are markers of oligodendrocyte development and myelin formation [3,4]. The so-called Golli-isoforms (denoted BG21, J37, and TP8 in the mouse) are expressed at highest levels in oligodendrocytes at intermediate stages of differentiation [3]. The Golli-isoforms promote migration and process extension, and enhance potassium-induced calcium influx, a phenomenon that is dependent on plasma membrane targeting [4–7]. Other cell and tissue types also express Golli-isoforms, where they appear to function as regulators in signal transduction events [8–10]. In this context, phosphorylation of BG21 by protein kinase C (PKC) has been observed in PMA-activated Jurkat cells (PMA is phorbol-12-myristate-13-acetate) [10].

One of the potential binding partners of the murine Golli-isoform BG21 has been identified by the yeast two-hybrid system, and has been called Golli-interacting protein (GIP, 261 amino acids) [11]. This GIP was shown to have a high degree of sequence similarity to the proteins from the family of small subunit RNA polymerase II C-terminal domain (RNAP2-CTD) phosphatases, particularly the small CTD-phosphatase SCP1:99% sequence identity with human SCP1 (hSCP1) [12]. In addition, murine GIP was shown to be co-expressed with Golli-proteins in the nuclei of granule cells and oligodendrocytes, and GIP mRNA expression followed the BG21 expression pattern in developing brains [11]. These two proteins were shown to co-immunoprecipitate from whole-cell lysates of neuronal PC12n and glial N19 cells, the latter being an immortalized cell line that closely resembles an immature oligodendrocyte. Finally, GIP was co-immunoprecipitated with BG21 and NLI (nuclear LIM interactor) from lysates of N19 cells transfected with

* Corresponding author. Fax: +1 519 837 1802.
E-mail address: gharauz@uoguelph.ca (G. Harauz).

http://dx.doi.org/10.1016/j.bbrc.2014.04.050
0006-291X/

NLI. It was suggested that Golli proteins, particularly BG21, might play a role in NLI-associated regulation of gene expression/transcription. *Henceforth, since murine GIP (mGIP) is equivalent to murine SCP1 (mSCP1), our compromise nomenclature is mSCP1/GIP.*

We have previously presented an optimised protocol for the over-expression and purification, under native conditions, of a truncated form of recombinant murine mSCP1/GIP, representing the conserved region of the sequence (residues Q77-G260, with a C-terminal hexa-histidine tag) [13]. We showed that rmBG21 (recombinant murine BG21 isoform) at concentrations below 6 μM enhanced enzymatic activity, but significantly inhibited enzymatic activity when its concentration was higher. The two proteins were cross-linked *in vitro* with glutaraldehyde and gel-shift assays showed that the interaction was equimolar and specific, but not particularly strong. It was not possible then to purify the full-length enzyme under native conditions because of solubility issues. We have since developed and optimised a new protocol for over-expressing and purifying the *full-length* recombinant mSCP1/GIP (without addition of any purification-facilitating tags), under native conditions, and in active form [14]. Here, the *in vitro* association of the full-length mSCP1/GIP with rmBG21 is investigated enzymatically, demonstrating for the first time that the N-terminus of mSCP1/GIP affects protein–protein interactions that modulate its phosphatase activity.

2. Materials and methods

2.1. Proteins and phosphorylation

Full-length mSCP1/GIP fused to SUMO at its N-terminus was cloned into the Champion™ pET SUMO Expression System (Invitrogen Life Technologies, Burlington, ON), and expressed in *Escherichia coli* BL21-CodonPlus(DE3)-RP cells [14]. The SUMO-fusion tag strategy was chosen to improve the expression and solubility of the enzyme [15,16]. The addition of 5 mM DTT (dithiothreitol) to the lysis procedure helped to solubilise the protein, likely by preventing non-specific aggregation via aberrant disulphide cross-links between lipid-associated proteins and the free cysteines in the N-terminus of mSCP1/GIP. Our new, optimised protocol yielded ~4–5 mg of active mSCP1/GIP per 1 L of cell culture on average [14].

Recombinant murine BG21 (rmBG21, hexa-histidine-tagged) was over-expressed in *E. coli* BL21-CodonPlus(DE3)-RP and purified as previously described [17,18]. It was phosphorylated *in vitro* with protein kinase Cα (PKCα) (Millipore, Temecula, CA) as follows. The mixture (total volume of 0.5 mL), containing 300 μg of rmBG21 was incubated with 1 μg PKCα at 30 °C for 4 h in the presence of 0.15 mM ATP, 10 mM $MgCl_2$, 0.2 mM $CaCl_2$, and PKC lipid activator (Millipore, Temecula, CA) in 20 mM HEPES–NaOH, pH 7.4. Phosphorylated proteins were separated from the remaining unmodified proteins by HPLC (high-performance liquid chromatography) using a Waters apparatus with a Symmetry 300 C18, 5 μm, 4.6 × 250 mm column as previously described (Fig. S1 of Supplementary Information) [16,18].

2.2. Phosphatase assays with the artificial p-NPP substrate

For the dephosphorylation of the artificial substrate *p*-NPP (*p*-nitrophenylphosphate) by full-length mSCP1/GIP, a standard discontinuous assay was used to detect the reaction product *p*-NP (*p*-nitrophenol) via its absorbance at 405 nm (A_{405}, ε = 18,300 M^{-1} cm^{-1}) [18]. Reaction mixtures were assembled in 50 mM Tris–acetate, pH 5.5, 10 mM $MgCl_2$, and increasing concentrations of the substrate *p*-NPP (0–15 mM) with a final volume of 100 μL. Mixtures were incubated at 37 °C for 5 min to stabilize the temperature. Reactions were initiated by the addition of 50 nM mSCP1/GIP (final concentration). After 10 min, 1 M NaOH (final concentration) was added to terminate the reaction and the absorbance at 405 nm was measured.

2.3. Inhibition/activation of full-length mSCP1/GIP by rmBG21 isoforms

The activity assay for full-length mSCP1/GIP was performed as above using the artificial substrate *p*-NPP at constant 10 mM concentration, but with increasing concentrations of rmBG21 (0–30 μM). A global fit of the equation below to the ensemble of velocity graphs was performed in order to obtain the inhibition or activation constants:

$$V = \frac{V_{max}\frac{[S]}{K_M} + \beta V_{max}\frac{[S][I]}{\alpha K_M K_I}}{1 + \frac{[S]}{K_M} + \frac{[I]}{K_I} + \frac{[S][I]}{\alpha K_M K_I}} \quad (1)$$

Here, α represents the cooperativity between the modulator, *I*, and the substrate, *S*; β represents the extent of inhibition or activation on the observed velocity, *V*, by the modulator; V_{max} is the maximal velocity of the enzyme in the absence of the modulator, and K_M is the concentration of substrate required to reach half of this value. Finally, K_I represents the inhibition or activation constant between the free enzyme and the modulator. The global fit was done using Microcal OriginPro version 8.0 (OriginLab, Northampton, MA), with α, β, and K_I as shared parameters across all experimental curves.

2.4. Phosphatase assays with the synthetic CTD-peptide as substrate

The CTD of RNAP2 comprises a number of heptad repeats and represents a natural substrate for mSCP1/GIP [19,20]. Here, a synthetic di-heptad CTD-peptide (14 residues, sequence YSPTSP-SYSPT-phosphoSer-PS) [19] was synthesized by Biomatik Corporation (Cambridge, ON). Reaction mixtures were combined in 50 mM Tris–acetate, pH 5.5, 10 mM $MgCl_2$, with increasing concentrations of synthetic CTD-peptide (0–90 μM) in a final volume of 50 μL. Mixtures were incubated at 37 °C for 5 min to stabilize the temperature. Reactions were initiated by the addition of 12.5 nM mSCP1/GIP. After 5 min, the reactions were terminated by boiling, and then frozen until developed. Under the same conditions, mSCP1/GIP was incubated at 12.5 nM with 90 μM of phosphorylated rmBG21. Reaction mixtures were incubated at 37 °C for 5 min, 0.5 h, and 24 h.

The dephosphorylation of the CTD-peptide by mSCP1/GIP was measured via a standard malachite green discontinuous assay [21]. Three parts of 0.045% malachite green in ddH_2O were combined with one part 4.2% ammonium molybdate in 4 M HCl to form the developing reagent. The reagent was then centrifuged at maximum speed for 10 min to remove any precipitates. The 50-μL reaction mixtures and phosphate standards (Sigma-Aldridge, Oakville, ON) were aliquoted into a 96-well plate, and a multi-channel pipette was used to add 100 μL of the developing reagent solution to all wells simultaneously. Absorbance at 620 nm (A_{620}) was then immediately measured. The phosphate standards were used to plot a standard curve (0–70 μM) in order to quantify the amount of inorganic phosphate present. All reactions were done in triplicate and repeated with several preparations of mSCP1/GIP.

Kinetic parameters with the natural CTD-peptide substrate, particularly the effects of unmodified and phosphorylated BG21, were determined as above for *p*-NPP.

3. Results

We have developed a new protocol for the purification of full-length mSCP1/GIP under native conditions, described in detail

elsewhere [14]. Circular dichroism spectroscopy of full-length mSCP1/GIP yielded spectra consistent with a well-folded protein with a high degree of α-helical structure (not shown). The kinetic parameters of this enzyme were characterised using the artificial substrate *p*-NPP and a discontinuous tube assay. Standard Michaelis–Menten modelling yielded a K_m of 4.57 ± 0.30 mM, and a k_{cat} of 3.95 ± 0.37 s^{-1}, which are favourably comparable to the values previously reported by us for truncated ΔN-rmSCP1/GIP [13], and to those reported by others for the truncated human orthologue ΔN-hSCP1 [22,23]. With the more natural CTD-peptide substrate and the malachite green assay for detection of inorganic phosphate released, the purified enzyme also displayed canonical Michaelis–Menten kinetics with a K_m of 69.5 ± 3.4 μM, and a k_{cat} of 2.44 ± 0.04 s^{-1}, also in good congruence with ΔN-hSCP1 [22]. Thus, this recombinant full-length enzyme preparation was functional. It was found that either freezing the bacterial cell pellet before lysis for storage, or a total purification time > 72 h, resulted in significantly reduced enzyme activity.

Next, an enzymatic approach was used to study potential modulatory interactions of rmBG21 with the enzyme, first with the artificial substrate *p*-NPP at fixed concentration while increasing the concentration of unmodified rmBG21. The velocity of the reaction recorded was normalised as a percentage of enzymatic activity of the catalysis in the absence of potential interacting protein. It was evident first that unmodified rmBG21 had an inhibitory effect on mSCP1/GIP phosphatase activity on the *p*-NPP substrate (Fig. 1A). The major drop in activity started with ~4 μM rmBG21, and saturation occurred at ~15 μM rmBG21, by which time enzymatic activity was reduced to 40%.

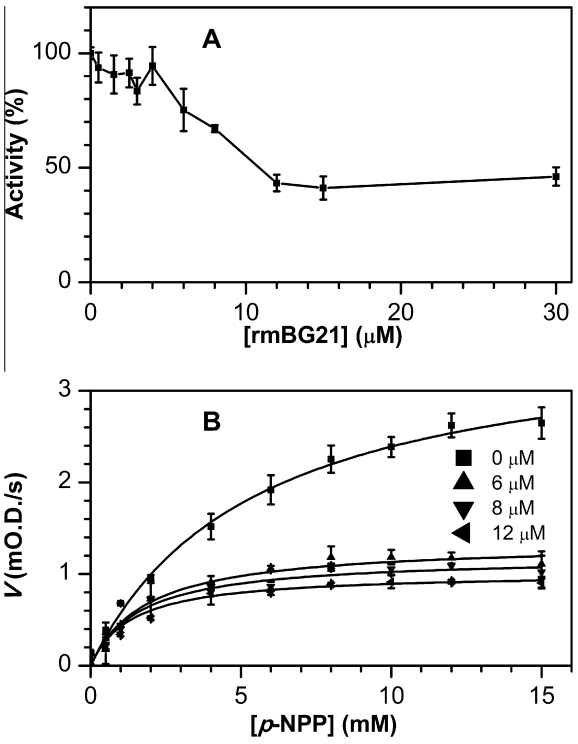

Fig. 1. Profile of the effect of unmodified rmBG21 on the phosphatase activity of full-length mSCP1/GIP using the artificial substrate *p*-NPP. (A) Effect of (0–30 μM) rmBG21 on mSCP1/GIP activity at constant *p*-NPP concentration (10 mM) (normalized to 100% in the absence of rmBG21). (B) Mechanism of rmBG21 inhibition of mSCP1/GIP activity on *p*-NPP (0–15 mM). This experiment was repeated with different concentrations of rmBG21 (0, 6, 8, 12 μM). Each of these experiments was done in triplicate, and repeated with two separate mSCP1/GIP preparations; error bars represent the standard deviation of three individual experiments. Data were fitted to the inhibition model (Eq. (1)) using a non-linear global fit in OriginPro 8.0. For comparison, Cornish-Bowden and Dixon plots of the curves in panel (B) are shown in Fig. S2 of Supplementary Information.

We next measured the velocity curves at 0, 6, 8, and 12 μM concentrations of unmodified rmBG21 as an inhibitor, still using *p*-NPP as a substrate in the 0–15 mM concentration range (Fig. 1B, Fig. S2 of Supplementary Information). The V_{max} decreased progressively with increasing concentrations of rmBG21. A global fit of the velocity curves to the inhibition model (Eq. (1)) yielded an α-value of 0.13 ± 0.01, a β-value of 0.16 ± 0.03, and an inhibitory constant of 14 ± 8.9 μM (Table 1).

This experiment was repeated using the CTD-peptide as a more natural substrate and the malachite green assay, still with unmodified rmBG21 (Fig. 2A, Fig. S3 of Supplementary Information). Interestingly, there was an enhancement of mSCP1/GIP activity by rmBG21. The global fit of these data revealed an α-value of 0.26 ± 0.07, a β-value of 1.08 ± 0.09, and an activation constant of 30 ± 12 μM (Table 1). Finally, the same experiment was performed with PKCα-phosphorylated rmBG21, which intriguingly *inhibited* dephosphorylation of the CTD-peptide substrate (Fig. 2B, Fig. S4 of Supplementary Information). The global fit revealed an α-value of 0.97 ± 0.3, a β-value of 0.08 ± 0.03, and an inhibitory constant of 2.9 ± 0.5 μM (Table 1). A previous control experiment had demonstrated that phospho-rmBG21 itself was not a substrate for mSCP1/GIP (results not shown) [14].

4. Discussion

Having achieved the preparation of functional, full-length mSCP1/GIP, the next question was whether the N-terminus on the protein affected its interactions with BG21, which had only previously been studied with the truncated ΔN-rmSCP1/GIP form of the enzyme [13]. When mSCP1/GIP was first identified as "Golli-interacting protein", strong interactions between mSCP1/GIP and the Golli-isoform BG21 were inferred from the co-immunoprecipitation data [11]. In later *in vitro* studies by our group, the truncated ΔN-rmSCP1/GIP and rmBG21 were shown to have a very weak, though still specific, interaction [13]. Moreover, rmBG21 was also shown to dually affect the ability of truncated ΔN-rmSCP1/GIP to catalyse *p*-NPP hydrolysis. Then, it was argued that the missing 76-residue unstructured N-terminus could be important in this interaction. Here in this present study, the latter experiment was repeated with full-length mSCP1/GIP, seeing how increasing concentrations of rmBG21 affect its enzymatic reaction with the artificial substrate *p*-NPP. As Fig. 1A shows, rmBG21 inhibited mSCP1/GIP to about 40% of its original activity. No dual effect was observed here as was seen earlier with the truncated form of the enzyme [18].

A more detailed analysis of this inhibition through a global fit to the mixed inhibition model described by Eq. (1)reveals a significant decrease in the ability of mSCP1/GIP to be able to bind and catalyse the substrate as shown by the hindered α- (0.13) and β- (0.16) values (Fig. 1B, Table 1). This result implies that although rmBG21 binds allosterically to mSCP1/GIP, its binding significantly disturbs the active site. A K_i value of 14 μM indicates a strong interaction between mSCP1/GIP and rmBG21. This conclusion is now in better agreement with the original co-immunoprecipitation studies [11]. This congruence now also provides evidence that the N-terminus of mSCP1/GIP helps to modulate the interaction with BG21.

Next, the rmBG21 inhibition experiment was repeated using the CTD-peptide substrate (Fig. 2). Unexpectedly, unmodified rmBG21 *enhances* the enzymatic activity of mSCP1/GIP towards the CTD-peptide (Table 1). The same mixed inhibition model was applied to analyse this mode of interaction, and showed that rmBG21 shifts the binding equilibrium towards the enzyme–substrate complex

Table 1
Summary of inhibition parameters of full-length mSCP1/GIP obtained with unmodified and phosphorylated variants of the Golli-isoform BG21, derived from global fits of velocity graphs to Eq. (1).

Inhibitor	Substrate	α	β	Inhibition/activation constant K_i (μM)
Unmodified rmBG21	*p*-NPP	0.13 ± 0.01	0.16 ± 0.03	14 ± 8.9
Unmodified rmBG21	CTD-peptide	0.26 ± 0.07	1.08 ± 0.09	30 ± 12
PKCα-phosphorylated rmBG21	CTD-peptide	0.97 ± 0.3	0.08 ± 0.03	2.9 ± 0.5

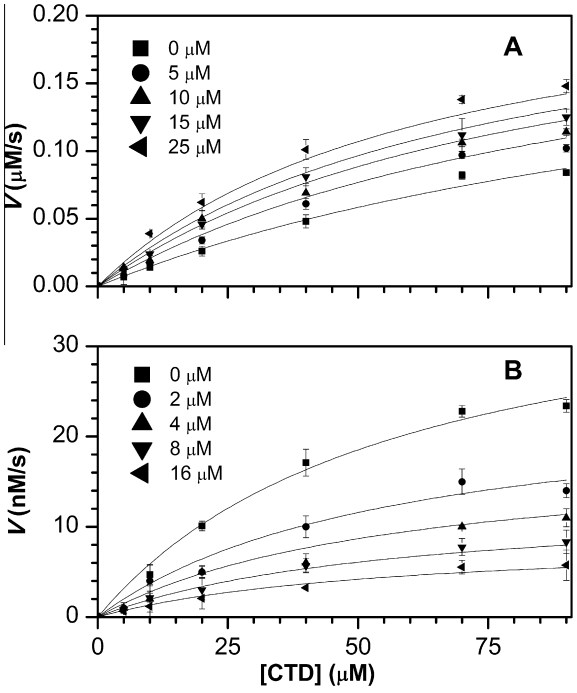

Fig. 2. Effect of unmodified and PKCα-phosphorylated rmBG21 on the mechanism of inhibition of mSCP1/GIP activity on CTD-peptide (0–90 μM) substrate. This experiment was repeated with different concentrations of (A) unmodified rmBG21 (0, 5, 10, 15, 25 μM), and (B) phosphorylated rmBG21 (0, 2, 4, 8, 16 μM), and was initiated by the addition of 50 nM and 12.5 nM mSCP1/GIP, respectively. Each of these experiments was done in triplicate, and repeated with two separate mSCP1/GIP preparations; error bars represent the standard deviation of three individual experiments. Data were fitted to Eq. (1) using a non-linear global fit in OriginPro 8.0. The data in panel (A) are shown in Lineweaver–Burke, Dixon, and Cornish-Bowden representations in Fig. S3 of the Supplementary Information. The data in panel (B) are shown in Dixon and Cornish-Bowden representations in Fig. S4 of the Supplementary Information.

($\alpha = 0.26$) while not affecting the ability of mSCP1/GIP to catalyse its substrate ($\beta = 1.08$). The interaction between mSCP1/GIP and rmBG21 also remains strong ($K_i = 30$ μM).

We interpret these observations using a general mixed inhibition model, illustrated schematically in Fig. 3. As the rmBG21 concentration is increased, rmBG21 and the CTD-peptide bind mSCP1/GIP. This results in an overall greater amount of apparent substrate that can be readily catalysed at the same rate, leading to the observed enhancement in activity. In contrast to the inhibition observed with the artificial substrate *p*-NPP, the active site does not appear to be disturbed with the CTD-peptide substrate. Both rmBG21 and the CTD-peptide are unstructured and conformationally adaptive to their surroundings, and it can be suggested that they do so when they bind mSCP1/GIP while leaving unchanged the residues involved in catalysis, namely D98.

Following this result, the same experiment was done with the PKCα-phosphorylated rmBG21 instead. The PKCα-phosphorylated rmBG21 has the opposite effect on mSCP1/GIP compared to unmodified rmBG21, *i.e.*, phospho-rmBG21 does not affect the binding equilibrium between mSCP1/GIP and the CTD substrate. However, it greatly decreases the ability of mSCP1/GIP to properly catalyse the CTD-peptide once bound, leading to an overall inhibition effect. Here, it seems that phospho-rmBG21 does not interact with the CTD-peptide when docking to mSCP1/GIP, but it does have a significant effect on the residues (like D98) involved in the hydrolysis step of the mechanism. Moreover, phosphorylation of rmBG21 significantly (10-fold) increases the strength of interaction between rmBG21 and mSCP1/GIP ($K_i = 2.9$ μM). This observation suggests that the phosphorylation of rmBG21 is an important molecular switch event ("quick-brake mechanism") in the regulation of mSCP1/GIP activity (Fig. 3). Once rmBG21 is phosphorylated by PKCα, it acts to inhibit the dephosphorylation of the CTD by mSCP1/GIP.

In summary, we conclude from these data that the N-terminus of mSCP1/GIP affects its interaction with BG21, which is an intrinsically-disordered protein (IDP) [24,25]. In general, IDPs are highly-extended and flexible, and often act as "hubs" in structural or signalling networks [26]. The interactions of IDPs with other biomolecules involve local disorder-to-order transitions, either by induced fit, or fixation of transient fluctuations that form recognisable target motifs, as exemplified by myelin proteins [27–30]. This plasticity that IDPs have is essential in many cell events such as gene regulation and differentiation [26,31]. The dual effect that BG21 has on mSCP1/GIP depending on its phosphorylation state could be another example of the new idea of "multisteric" regulation as an extension to IDPs of the traditional concept of allostery (*cf.*, [31]), and suggests a potential functional role for these two proteins' interaction in regulating the development and

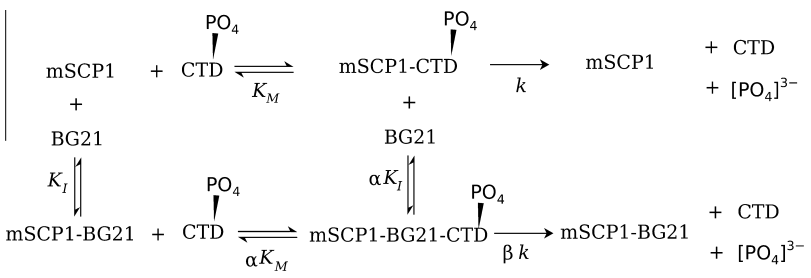

Fig. 3. Schematic representation of a general mixed inhibition mechanism where the binding of BG21 (modulator) to mSCP1/GIP (enzyme) is described by K_I, whereas K_M represents the binding of the CTD-peptide (substrate) to mSCP1/GIP. These two constants are linked by a cooperativity factor, α. The rate of the catalysis of CTD-peptide, k, is affected by the modulator according to the β-factor.

maturation of the oligodendrocyte. These interactions may also occur outside of the central nervous system, given that BG21 is the main Golli-protein present in T-cells: here it has been shown to be a substrate for PKC, acting as a negative regulator of its pathway to regulate the T-cell receptor and its antigen recognition sensitivity [10].

Acknowledgments

This work was supported by the Natural Sciences and Engineering Research Council of Canada (NSERC Discovery Grant RG121541 to G.H.). K.A.V. was the recipient of a Post-Doctoral Fellowship from the Multiple Sclerosis Society of Canada. G.H. is also grateful to the Canada Research Chairs Program. Drs. Anthony and Celia Campagnoni (Neuropsychiatric Institute, University of California at Los Angeles) provided the original mGIP (mSCP1) clone. The pET28b plasmid encoding recombinant SUMO protease was a gift from Dr. Christopher Lima (Sloan-Kettering Institute, NY). The authors are further grateful to Drs. Rod Merrill and Miguel Lugo (Guelph) for invaluable advice and many helpful discussions.

The authors have no conflict of interests to declare.

Appendix A. Supplementary data

Supplementary data associated with this article can be found, in the online version, at http://dx.doi.org/10.1016/j.bbrc.2014.04.050.

References

[1] V.E. Miron, T. Kuhlmann, J.P. Antel, Cells of the oligodendroglial lineage, myelination, and remyelination, Biochim. Biophys. Acta 2011 (1812) 184–193.
[2] N. Snaidero, W. Mobius, T. Czopka, L.H. Hekking, C. Mathisen, D. Verkleij, S. Goebbels, J. Edgar, D. Merkler, D.A. Lyons, K.A. Nave, M. Simons, Myelin membrane wrapping of CNS axons by PI(3,4,5)P3-dependent polarized growth at the inner tongue, Cell 156 (2014) 277–290.
[3] M.I. Givogri, E.R. Bongarzone, V. Schonmann, A.T. Campagnoni, Expression and regulation of golli products of myelin basic protein gene during *in vitro* development of oligodendrocytes, J. Neurosci. Res. 66 (2001) 679–690.
[4] D. Fulton, P.M. Paez, A.T. Campagnoni, The multiple roles of myelin protein genes during the development of the oligodendrocyte, ASN Neuro 2 (2010). e00027-25–e00027-37.
[5] P.M. Paez, D.J. Fulton, V. Spreuer, V. Handley, C.W. Campagnoni, A.T. Campagnoni, Regulation of store-operated and voltage-operated Ca++ channels in the proliferation and death of oligodendrocyte precursor cells by Golli proteins, ASN Neuro 1 (2009). e00003-25–e00003-41.
[6] P.M. Paez, D.J. Fulton, V. Spreuer, V. Handley, C.W. Campagnoni, W.B. Macklin, C. Colwell, A.T. Campagnoni, Golli myelin basic proteins regulate oligodendroglial progenitor cell migration through voltage-gated Ca2+ influx, J. Neurosci. 29 (2009) 6663–6676.
[7] D. Fulton, P.M. Paez, R. Fisher, V. Handley, C.S. Colwell, A.T. Campagnoni, Regulation of L-type Ca(++) currents and process morphology in white matter oligodendrocyte precursor cells by golli-myelin proteins, Glia 58 (2010) 1292–1303.
[8] M.I. Givogri, E.R. Bongarzone, A.T. Campagnoni, New insights on the biology of myelin basic protein gene: The neural-immune connection, J. Neurosci. Res. 59 (2000) 153–159.
[9] J.M. Feng, A.O. Fernandes, A.T. Campagnoni, Golli-myelin basic proteins delineate the nerve distribution of lymphoid organs, J. Neuroimmunol. 123 (2002) 1–8.
[10] J.M. Feng, A.O. Fernandes, C.W. Campagnoni, Y.H. Hu, A.T. Campagnoni, The golli-myelin basic protein negatively regulates signal transduction in T lymphocytes, J. Neuroimmunol. 152 (2004) 57–66.
[11] A.O. Fernandes, C.W. Campagnoni, K. Kampf, J.M. Feng, V.W. Handley, V. Schonmann, E.R. Bongarzone, S. Reyes, A.T. Campagnoni, Identification of a protein that interacts with the golli-myelin basic protein and with nuclear LIM interactor in the nervous system, J. Neurosci. Res. 75 (2004) 461–471.
[12] M. Yeo, P.S. Lin, M.E. Dahmus, G.N. Gill, A novel RNA polymerase II C-terminal domain phosphatase that preferentially dephosphorylates serine 5, J. Biol. Chem. 278 (2003) 26078–26085.
[13] V.V. Bamm, G. Harauz, Expression and purification of the active variant of recombinant murine Golli-interacting protein (GIP) – characterization of its phosphatase activity and interaction with Golli-BG21, Protein Expr. Purif. 62 (2008) 36–43.
[14] S. Jaramillo-Tatis, Characterization of the Golli-Interacting Protein and its Interactions with BG21 and the 21.5-kDa Isoform of Myelin Basic Protein (M.Sc. Thesis), Department of Molecular and Cellular Biology, University of Guelph, Canada, 2013. <https://atrium.lib.uoguelph.ca/xmlui/handle/10214/7570>.
[15] L.N. Rahman, G.S.T. Smith, V.V. Bamm, J.A. Voyer-Grant, B.A. Moffatt, J.R. Dutcher, G. Harauz, Phosphorylation of *Thellungiella salsuginea* dehydrins TsDHN-1 and TsDHN-2 facilitates cation-induced conformational changes and actin assembly, Biochemistry 50 (2011) 9587–9604.
[16] V.V. Bamm, M. De Avila, G.S.T. Smith, M.A. Ahmed, G. Harauz, Structured functional domains of myelin basic protein: cross talk between actin polymerization and Ca(2+)-dependent calmodulin interaction, Biophys. J. 101 (2011) 1248–1256.
[17] M.A.M. Ahmed, V.V. Bamm, G. Harauz, V. Ladizhansky, The BG21 isoform of Golli myelin basic protein is intrinsically disordered with a highly flexible amino-terminal domain, Biochemistry 46 (2007) 9700–9712.
[18] V.V. Bamm, M.A. Ahmed, V. Ladizhansky, G. Harauz, Purification and spectroscopic characterization of the recombinant BG21 isoform of murine golli myelin basic protein, J. Neurosci. Res. 85 (2007) 272–284.
[19] S.R. Peterson, A. Dvir, C.W. Anderson, W.S. Dynan, DNA binding provides a signal for phosphorylation of the RNA polymerase II heptapeptide repeats, Genes Dev. 6 (1992) 426–438.
[20] D. Eick, M. Geyer, The RNA polymerase II carboxy-terminal domain (CTD) code, Chem. Rev. 113 (2013) 8456–8490.
[21] T.P. Geladopoulos, T.G. Sotiroudis, A.E. Evangelopoulos, A malachite green colorimetric assay for protein phosphatase activity, Anal. Biochem. 192 (1991) 112–116.
[22] M. Zhang, J. Liu, Y. Kim, J.E. Dixon, S.L. Pfaff, G.N. Gill, J.P. Noel, Y. Zhang, Structural and functional analysis of the phosphoryl transfer reaction mediated by the human small C-terminal domain phosphatase, Scp1, Protein Sci. 19 (2010) 974–986.
[23] Y. Zhang, Y. Kim, N. Genoud, J. Gao, J.W. Kelly, S.L. Pfaff, G.N. Gill, J.E. Dixon, J.P. Noel, Determinants for dephosphorylation of the RNA polymerase II C-terminal domain by Scp1, Mol. Cell 24 (2006) 759–770.
[24] C.M.D. Hill, I.R. Bates, G.F. White, F.R. Hallett, G. Harauz, Effects of the osmolyte trimethylamine-*N*-oxide on conformation, self-association, and two-dimensional crystallization of myelin basic protein, J. Struct. Biol. 139 (2002) 13–26.
[25] G. Harauz, N. Ishiyama, C.M.D. Hill, I.R. Bates, D.S. Libich, C. Farès, Myelin basic protein – diverse conformational states of an intrinsically unstructured protein and its roles in myelin assembly and multiple sclerosis, Micron 35 (2004) 503–542.
[26] V.N. Uversky, The mysterious unfoldome: structureless, underappreciated, yet vital part of any given proteome, J. Biomed. Biotechnol. 2010 (2010) 568068.
[27] G. Harauz, V. Ladizhansky, J.M. Boggs, Structural polymorphism and multifunctionality of myelin basic protein, Biochemistry 48 (2009) 8094–8104.
[28] D.S. Libich, M.A. Ahmed, L. Zhong, V.V. Bamm, V. Ladizhansky, G. Harauz, Fuzzy complexes of myelin basic protein: NMR spectroscopic investigations of a polymorphic organizational linker of the central nervous system, Biochem. Cell Biol. (Special Issue on Protein Folding: Principles and Diseases) 88 (2010) 143–155.
[29] G. Harauz, D.S. Libich, E. Polverini, K.A. Vassall, The classic protein of myelin – conserved structural motifs and the dynamic molecular barcode involved in membrane adhesion, protein–protein interactions, and pathogenesis in multiple sclerosis, in: B.M. Dunn (Ed.), Advances in Protein and Peptide Science, Bentham Science Publishers, 2013, pp. 1–53 (e-book). <http://benthamscience.com/ebooks/9781608054879/index.htm>.
[30] K.A. Vassall, K. Bessonov, M. De Avila, E. Polverini, G. Harauz, The effects of threonine phosphorylation on the stability and dynamics of the central molecular switch region of 18.5-kDa myelin basic protein, PLoS One 8 (2013). e68175-1–e68175-19.
[31] P. Tompa, Multisteric regulation by structural disorder in modular signaling proteins: an extension of the concept of allostery, Chem. Rev. (2014) (in press). http://dx.doi.org/10.1021/cr4005082.